

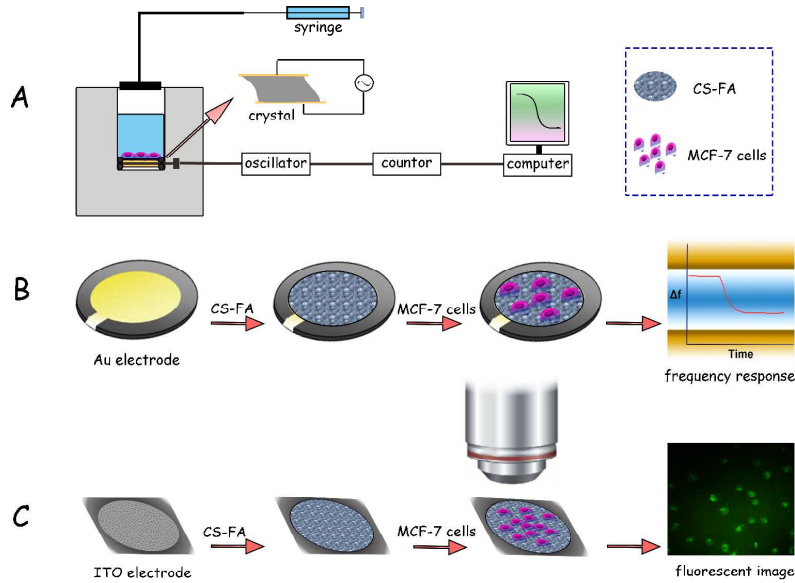


A recyclable chitosan - based QCM biosensor for sensitive and selective detection of breast cancer cells in real time

| | |
|-------------------------------|---|
| Journal: | <i>Analyst</i> |
| Manuscript ID: | AN-ART-08-2014-001532.R1 |
| Article Type: | Paper |
| Date Submitted by the Author: | 15-Sep-2014 |
| Complete List of Authors: | Zhang, Shaolian; Ji Nan university, Bai, Haihua; Jinan university, Luo, Jinmei; Jinan university, yang, Pei; jinan university, chemistry Cai, Jiye; jinan university, chemistry; State Key Laboratory of Quality Research in Chinese Medicines, Macau University of Science and Technology, |
| | |

Graphic abstract

A sensitive and recyclable QCM biosensor for the real-time measurement of MCF-7 breast cancer cell was developed for the first time using folic acid coupled to chitosan as an excellent biocompatibility biosensor film.



1
2
3
4
5
6
7
8
9
10
11
12
13
14
15
16
17
18
19
20
21
22
23
24
25
26
27
28
29
30
31
32
33
34
35
36
37
38
39
40
41
42
43
44
45
46
47
48
49
50
51
52
53
54
55
56
57
58
59
60

1
2
3
4
5
6
7 **A recyclable chitosan - based QCM biosensor for sensitive and**
8 **selective detection of breast cancer cells in real time**
9

10
11
12
13
14 Shaolian Zhang¹, Haihua Bai¹, Jinmei Luo¹, Peihui Yang^{1*}, Jiye Cai^{1,2}

- 15
16
17 *1. Department of Chemistry, Jinan University, Guangzhou 510632, People's*
18 *Republic of China*
19
20 *2. State Key Laboratory of Quality Research in Chinese Medicines, Macau University of*
21 *Science and Technology, Macau, China*
22
23
24
25
26
27
28
29

30 *Corresponding author:

31 Peihui Yang, Ph.D, Professor

32 Department of Chemistry, Jinan University

33 Guangzhou 510632, China

34 E-mail address: typh@jnu.edu.cn

35 Tel/Fax: +86-20-85223569

36
37
38
39
40
41
42
43 Shaolian Zhang: zhangshaolian1990@163.com
44
45
46
47
48
49
50
51
52
53
54
55
56
57
58
59
60

Abstract

A highly sensitive and recyclable quartz crystal microbalance QCM biosensor was developed using chitosan (CS) and folic acid (FA), generating conjugates that are selectively recognized by MCF-7 cancer cells over-expressed folic acid receptors. The prepared CS-FA conjugation was characterized with UV-vis spectroscopy and Fourier transform infrared spectroscopy. Atomic force microscopy and scanning electron microscopy further presented the morphology of the CS-FA conjugation interface. The hydrophilicity of films was characterized by measuring the contact angle. The recognition of MCF-7 cancer cells was investigated in situ using QCM. Captured by FA, MCF-7 cell was determined on-line using quartz crystal microbalance and a wide linear range of 4.5×10^2 - 1.01×10^5 cells mL⁻¹ was obtained, with a detection limit of 430 cells mL⁻¹. Fluorescence microscope further confirmed the specificity and biocompatibility of the constructed biosensor. In addition, the regeneration of the QCM biosensor was studied by using lysozyme. This receptor-bound ligand based QCM biosensor also showed good selectivity, repeatability in cell mixture. For the first time, this simple, economical and label-free chitosan-based QCM sensing was demonstrated, and such design could provide a promising detection strategy for sensitive detection of cancer cells over-expressed folic acid receptors.

Keywords: Quartz crystal microbalance; Chitosan; Folic acid; real time; recyclable; Breast cancer cell

1. Introduction

Nowadays, breast cancer is the most common women's cancer worldwide. Development of early detection techniques for breast cancer is primarily important for improving survival rates.^{1, 2} Conventional diagnostic methods, including polymerase chain reaction (PCR)-based methods,^{3, 4} cytometric methods,⁵ and cell-enrichment⁶ have been developed for cancer cell analysis. Although they have a high detection rate, many of these methods are expensive and time-consuming. They also require advanced instrumentation and enrichment of the target cells in the sample or expression of protein biomarkers or antibodies in the cells. Therefore, the developments of simple, time-saving, convenient and more economical methods for cancer cell detection are still needed.

The most recent efforts in cancer cell detection have focused on biosensors with good sensitivity and selectivity, as well as rapid and easy operation. Various biosensors using different transducers have been reported as effective in detecting and identifying cancer cell, including those based on electrochemical measurement,⁷⁻¹² fluorescence measurement,^{13, 14} single nanotube field effect transistor array,¹⁵ microfluidic devices.¹⁶ Although many of them have been applied at the laboratory research level, they are difficult to regeneration or suffer from time-consuming steps for labeling or off-line analysis. Hence, constructing a biosensor that avoids labor-intensive labeling steps and can be regeneration and allows real-time, on-line analysis is of great importance for simple and rapid cell analysis.

Alternatively, more attention has been paid to quartz crystal microbalance (QCM) as a sensor due to its rapid analysis speed, satisfactory sensitivity, simple instrumentation, and low cost.^{17, 18} QCM is a non-invasive, real-time and label-free technology that has been applied in many cell researches such as attachment, adhesion and spreading of cells on diverse kinds of coating layers.¹⁹⁻²¹ The QCM technique can also detect the cellular responses to drugs²² and exogenous stimulations,²³ nanoparticle,²⁴ or microparticle.⁶ The advantages of QCM in these studies are that it can be used as a continuous monitoring device and can detect cumulative effects in a

1
2
3 non-invasive way with high sensitivity. However, only a few references have reported
4 the detection of cancer cells via QCM. Pan *et al.*⁶ proposed a method for collection
5 and detection of leukemia cells on a magnet-quartz crystal microbalance system using
6 aptamer-conjugated magnetic beads, but this method suffer from time-consuming
7 steps for collection of cells. Shan *et al.*¹⁷ developed an aptamer-based QCM biosensor
8 for detection of leukemia cells, but the artificial aptamer is expensive and difficult to
9 regeneration after immobilized on the QCM sensor surface. Nevertheless, QCM
10 cytosensors are still in the development phase, the key is to develop a recyclable
11 functionalized biosensor interface with good biocompatibility for selective
12 recognition and capture of target cancer cells.
13
14
15
16
17
18
19
20
21

22 Thus, choosing interface materials was the critical step in the preparation of a
23 recyclable functionalized biosensor. Chitosan (CS), an abundant natural biological
24 macromolecule in the world, has attracted high consideration due to its nontoxicity,
25 biocompatibility and biodegradability.²⁵ Much attention has been attracted to
26 CS-based biomedical materials and their applications in tissue engineering.^{26, 27} Up to
27 now, many chitosan-based QCM cytosensors have been reported to study cell
28 adhesion,^{28, 29} however, few reports has been focus on using chemical coupling
29 functional chitosan in cancer cell detection filed. Therefore, In order to make the
30 sensor specific for cancer cell, the CS was functionalized with folic acid (FA). FA can
31 specifically target folate receptors (FR), which are the protein receptors on the surface
32 of cell membrane and usually over-expressed on some tumor cells.³⁰ Such design
33 extends the application of chitosan in QCM biosensor, providing a promising
34 approach for the development of QCM cytosensor.
35
36
37
38
39
40
41
42
43
44
45

46 In this study, we conjugated FA with water soluble low molecular weight
47 chitosan for the fabrication of bio-functional interface on gold substrates for the first
48 time. Due to the folic acid can specifically recognize folate receptor over-expressed
49 on MCF-7 cancer cells membrane and then capture the MCF-7 cancer cells, thus high
50 selectivity for tumor cells can be obtained in comparison with normal cells in the
51 fabricated chitosan-based QCM cytosensors. We demonstrate that the as-prepared
52 cytosensor has a sensitive response to MCF-7 cells with a detection limit of 430 cells
53
54
55
56
57
58
59
60

1
2
3 mL⁻¹, above all, this prepared chitosan-based QCM biosensor shows good
4 regeneration, reproducibility and stability, which offering a new avenue to chitosan
5 applications in QCM cytosensing and other bioassay. In addition, the MCF-7 standard
6 spiked blood sample was determined to explore the potential of this method in
7 practical application. The method is simple, convenient and economical for breast
8 cancer cell detection, and has the potential for other cancer cells detection as well.
9
10
11
12
13
14
15

16 **2. Material and methods**

17 2.1. Reagent and material

18
19
20 Human breast cancer cell lines MCF-7, Human umbilical vein endothelial cells
21 (HUVEC), oral epithelial cell lines H376 were obtained from Institute of Physiology,
22 Jinan University. RPMI 1640 medium, EGM-2 medium, Eagle's medium
23 (DMEM)/Hams F12 nutrient, and fetal bovine serum (FBS) were purchased from
24 Gibco Co. Chitosan (CS, deacetylation degree of 85% and molecular weight of 37.6
25 KDa) was purchased from Golden-shell Biochemical Co., Ltd. Folic acid (FA),
26 1-(3-dimethylaminopropyl)-3-ethylcarbodiimide hydrochloride (EDC),
27 N-hydroxysuccinimide (NHS), bovine serum albumin (BSA) were obtained from
28 Sigma-Aldrich. Phosphate-buffered saline (PBS) solution consisting of 136.7 mmol
29 L⁻¹ NaCl, 2.7 mmol L⁻¹ KCl, 9.7 mmol L⁻¹ Na₂HPO₄ and 1.5 mmol L⁻¹ KH₂PO₄ was
30 used. All other reagents are analytical reagents. Nanopure deionized and distilled
31 water (18.2 MΩ) was used throughout all experiments.
32
33
34
35
36
37
38
39
40
41
42

43 2.2. Apparatus and characterizations

44
45 AT-cut 5 MHz quartz crystals (14 mm diameter) with gold electrode (10 mm
46 diameter) formed uniformly on one side was used. The resonant frequency of a quartz
47 crystal was measured with a KSV QCM-Z500 quartz crystal microbalance system
48 (KSV Instrument Ltd., Finland). The data recorded by QCM were analyzed by
49 QcmZBrowse software. The ultraviolet-visible (UV-vis) absorption spectra were
50 recorded with a UV-1901 UV-vis spectrophotometer (Beijing, China). Fourier
51 transform infrared spectroscopy (FT-IR) analyses were used on a Nicolet 6700 FT-IR
52 spectrometer (Nicolet, USA). Water contact angle measurements were performed
53
54
55
56
57
58
59
60

1
2
3 using a contact angle meter (CAM-PLUS; TANTEC company, German) at room
4 temperature. 5 μ L water droplet was used to experiment by the sessile drop method,
5
6 the reported values of the contact angle were the averages of five measurements at
7
8 different positions of the same sample in this paper. The morphology of the films was
9
10 characterized by scanning electron microscopy (SEM) (JEOL-JSM-6700F) and an
11
12 AutoProbe CP Research atomic force microscopy (AFM, Veeco, USA) in tapping
13
14 mode. Fluorescent images were acquired on a Nikon inverted microscopy (ECLIPSE
15
16 TE-2000U, Nikon Corporation, Japan) equipped with a video camera (DS-U1, Nikon
17
18 Corporation, Japan).

20 2.3. Synthesis of CS-FA

21
22 The conjugation of CS-FA was synthesized according to Mansouri's method,³¹
23
24 Briefly, FA in anhydrous DMSO was prepared by stirring at room temperature until
25
26 FA was well dissolved. Then, 0.4M EDC and 0.1M NHS were added and kept for 3 h
27
28 at 4 °C. In this step, an amount of mixture solution of EDC and NHS was added to the
29
30 above solution to activate the carboxyl of FA and form an NHS ester. It was then
31
32 added to a solution of 1% (w/v) chitosan (MW: 150 kDa) in acetate buffer (pH 4.7).
33
34 The active NHS ester was replaced by the primary amines presented in the chitosan,
35
36 and the chitosan were thus immobilized through the amide bond. The resulting
37
38 mixture was stirred at room temperature in the dark for 16 h. It was brought to pH 9.0
39
40 by drop wise addition of diluted aqueous NaOH and dialyzed first against phosphate
41
42 buffer pH 7.4 for 3 days and then against water for 3 days.

43 2.4. Cell culture

44
45 The MCF-7 cell culture conditions followed the reported protocols.³² Briefly,
46
47 human breast cancer cell lines MCF-7 were grown in RPMI 1640 culture media
48
49 supplemented with 100U/ml streptomycin, 100U/ml penicillin and 10% fetal bovine
50
51 serum at 37 °C in a humidified atmosphere of 5% CO₂. Erythrocytes were separated
52
53 from whole blood by centrifugation (3000 \times g, 10 min) and then washed three times
54
55 with PBS buffered solution.

56
57 Human umbilical vein endothelial cells (HUVEC) were cultured as described
58
59 previously.³³ In brief, HUVEC were cultured in flasks at 37 °C in a CO₂ (5%)
60

1
2
3 incubator. Once the cells reached 80% confluence, they were sub-cultured in 35mm
4 petri dishes (Greiner) pre-coated with gelatin from fish skin (Sigma) and grown to
5
6
7 confluence.

8
9 Oral epithelial cell lines H376 were cultured as the reported protocols.³⁴ Cells
10 were cultured at 37 °C and 5% (v/v) CO₂ in Dulbecco's modified Eagle's medium
11 (DMEM)/Hams F12 nutrient mix with 1 µg/L glucose supplemented with 10% (v/v)
12 heat-inactivated foetal calf serum, 20 mM l-glutamine, 0.5 g/mL hydrocortisone
13 (Sigma–Aldrich, UK) and 2500 IU/mL penicillin and streptomycin.

18 2.5. Fluorescent and MCF-7 cell image

19
20 ITO glass was chosen as a substrate in the fabrication of biosensor. After
21 successive sonication in ethanol, acetone and deionized water, ITO was rinsed with
22 deionized water and dried at room temperature. Similar modification on ITO was
23 carried out as that of QCM. Thus the prepared CS-FA/Au was immersed into 100 µL
24 of 10.0 mg mL⁻¹ BSA solution at 4 °C for 1 h to block active sites, carefully rinsed
25 with PBS (pH=7.4) and dried at room temperature. Then the modified ITO was
26 immersed into the cell suspension at 4 °C for 2 h, washed thoroughly with PBS again,
27 and finally dropped with 100 µL calcein-AM for 10 min. Images were taken by a
28 Nikon inverted microscopy. Excitations and filters were as follows: excitation filter
29 405 nm, LP 430 nm filter.

30 2.6. QCM measurements

31
32 All binding process was monitored on-line by using a KSV QCM-Z500
33 instrument at 25 °C with a flow rate of 200 µL/min. Prior to modification, crystal
34 chips (5 MHz, AT-cut) (QX 301, Q-Sense AB, Sweden) used were immersed in a
35 boiling solution (30% H₂O₂, 28 % ammonia, and deionized water in a volume ratio of
36 1:1:5) for 5 min. The washed chips were then rinsed thoroughly with deionized water,
37 dried by nitrogen gas prior to use.

38
39 The conjugation of CS-FA prepared above was spin-coated to the cleaned QCM
40 gold electrode, dried in a silica gel desiccator, and then quartz crystal was fixed to the
41 QCM chamber. The obtained modified chip was thoroughly rinsed with PBS buffer
42 and then used as the sensor surface for MCF-7 cell determination. MCF-7 cell sample
43
44
45
46
47
48
49
50
51
52
53
54
55
56
57
58
59
60

1
2
3 was injected to the QCM chamber for direct analysis, followed by rinsing with PBS
4 buffer solution to remove non-bound cells. Scheme 1 shows the schematic diagram of
5 preparation of the QCM biosensor.
6
7

8 9 2.7. Data analysis

10 The frequency and dissipation changes were monitored by instruments of QCM,
11 data analysis was performed using QcmZBwse software from Q-Sense.
12
13
14
15

16 17 3. Results and discussion

18 19 3.1. Characterization of CS-FA

20 The functionalized CS (CS-FA), CS and glass side were characterized using
21 AFM and SEM and as shown in Fig. 1. Fig. 1A shows the AFM images obtained for
22 CS-FA, CS and glass side, respectively. It was found that the roughness of the CS-FA
23 film is higher than the CS, suggesting that the CS-FA interface is getting rougher and
24 the surface area is increasing so that more MCF-7 cells can be recognized. Fig. 1B
25 also shows the images of an additional characterization of the film surface by SEM.
26 The image of CS-FA in Fig. 1B reveals the cross-linked structure of CS-FA, which
27 also confirmed the AFM image. The results for the control (glass slide) are also
28 shown for the sake of comparison. The above images revealed that FA was
29 successfully coupled to CS.
30
31
32
33
34
35
36
37
38

39 Fig. 2A shows the UV-vis absorption spectra of CS, FA and FA-CS, respectively.
40 In the case of CS, the extremely weak absorption peak corresponding to $n \rightarrow \pi^*$
41 transition shifted to 300 nm. For FA, two absorption peaks were observed, one was at
42 280 nm, corresponding to $\pi \rightarrow \pi^*$ transition of the C=C bond, and the other was at 360
43 nm, corresponding to $n \rightarrow \pi^*$ transition of the C=O bond. Whereas FA-CS has a
44 strong absorption peak at 280 nm and a weak absorption peak at 360 nm, which
45 confirmed the successful conjugation of FA with CS.^{35,36}
46
47
48
49
50
51

52 The FT-IR was further performed for the confirmation of the FA coupled to CS
53 successfully. Fig. 2B shows the FT-IR spectra of CS, FA and FA-CS composite
54 respectively. From Fig. 2B, All specimens show the characteristic peak at 1420 and ~
55 3400 cm^{-1} , which was attributed to the flexural vibration of CH_2 and stretching
56
57
58
59
60

1
2
3 vibration of N-H, respectively.³⁷ The FT-IR spectra of CS shows two bands located at
4 around 1638 cm⁻¹ and 1596 cm⁻¹ which could be assigned to amino I and amino II
5 functional groups of the native CS, respectively.²⁷ The binds observed at 1693 cm⁻¹
6 and ~ 1608 cm⁻¹ of FA corresponds to the C=O stretching vibration and the N-H
7 deformation.³⁸ CS-FA exhibits more distinctive bands associated with FA conjugation,
8 amide I and amide II at 1648 and 1565 cm⁻¹, and -OH stretching and N-H stretching
9 vibration centred at ~ 3360 cm⁻¹. The C=O stretching band of residual COOH of
10 conjugated FA was not noted, but it may overlay with the amide I, as occurred in
11 native FA.^{35,39}

12
13
14
15
16
17
18
19
20
21 The surface nature of materials, such as the surface charge, hydrophilicity and
22 wettability, is important for cell attachment or proliferation.⁴⁰ The hydrophilicity of
23 films was characterized by measuring the contact angle. As shown in Fig. 2C, the
24 corresponding contact angles for bare Au, CS and CS-FA were 42.0°, 78.2° and 48.4°,
25 respectively. Compared to CS, CS-FA had better hydrophilicity which was in favor of
26 enhancing cells loading and retaining their bioactivity. The CS-FA film showed the
27 lower contact angle, indicating the best hydrophilicity, attributed to the carboxyl and
28 hydroxyl groups in FA and CS. The results showed that the film could provide a
29 biocompatible surface and promote cell adhesion and growth.

30
31
32
33
34
35
36
37
38 The recognition of 1×10⁵ cells/mL MCF-7 cancer cells and HUVEC
39 non-cancerous cells were investigated in real-time using QCM technique (Fig. 2D).
40 For graphical simplification, the results in this figure present frequency (Δf) shift and
41 energy dissipation (ΔD) changes as a function of time for the 3th harmonic. As shown
42 in Fig. 2D, $\Delta f/v$ values of MCF-7 cells (curve d) captured by the biosensor were 3
43 times greater than those of HUVEC signals (curve c). This is due to the
44 over-expression of FR molecules on the MCF-7 cell surface and then specific
45 recognition by the biosensor, thus, the binding of cells to the FA
46 molecule-functionalized biosensor further added the mass on the oscillating quartz
47 crystal sensor, leading to a remarkable frequency decreases. Regarding energy
48 dissipation factor, ΔD , characterizes the viscoelasticity of the attached layer formed on
49
50
51
52
53
54
55
56
57
58
59
60

1
2
3 top of the sensing surface. ΔD is defined as the ratio of the dissipated energy and the
4 energy elastically stored per cycle.⁴¹ As can be observed from curve a in Fig. 2D, the
5 injection of MCF-7 cells causes a dissipation increase due to the viscoelastic nature of
6 the adsorbed cell layer, like the typical of polymeric systems. Interestingly, none or
7 very low ΔD signals was obtained by the biosensor in the non-cancerous cells (curve
8 b). This might be due to the less expression of FR molecule on the non-cancerous cell
9 surface, FA-functionalized sensor surface trapped less HUVEC cells, leading to low
10 dissipation shift. When rising with PBS buffer solution after recognition, an increase
11 in $\Delta f/v$ and slightly decrease in ΔD were observed due to the rinsing of non-specific
12 adsorption. According to the remarkably different QCM signals of cancer and
13 non-cancerous cells, it could be indicated that the amount of folic acid receptors
14 expressed on cancer cells surfaces were different from non-cancerous cells.
15
16
17
18
19
20
21
22
23
24
25

26 3.2. Optimization of synthesis of CS-FA

27
28 In this work, the QCM frequency signal intensity of the MCF-7 cells captured by
29 CS-FA interface was determined by the amount of FA in the conjugation. Thus,
30 optimization of the reaction conditions is necessary to plot the calibration curve, and
31 as shown in Fig. 3A, the degree of increasing of absorption intensity was linearly
32 related with the concentration of FA. They all have an excitation band at
33 approximately 280 nm, similar to the conjugate band. The influence of the FA
34 concentration on the maximum UV-vis absorption intensity was investigated by using
35 different mass ratio of CS to FA. Fig. 3B shows that the absorption intensity increased
36 with an increased FA ratio and tended to be constant beyond 1:4 ($M_{CS} : M_{FA}$). Over the
37 ratio of 1:4, the absorption intensity did not change significantly due to the saturation
38 effect. The error bars represent the standard deviation (S.D.) of three measurements.
39 Hence, the optimal mass ratio of CS to FA was 1:4.
40
41
42
43
44
45
46
47
48
49

50 3.3. Analytical performance of QCM biosensor

51
52 To evaluate the sensitivity and quantitative range of the proposed assay strategy,
53 the novel assay format was employed to detect different concentration of MCF-7 cells.
54 It can be seen (Fig. 4) that the QCM frequency responses for 7th harmonic increases
55 accordingly as the concentration of MCF-7 is varied from 450 cells/mL to 1.01×10^5
56
57
58
59
60

1
2
3
4
5
6
7
8
9
10
11
12
13
14
15
16
17
18
19
20
21
22
23
24
25
26
27
28
29
30
31
32
33
34
35
36
37
38
39
40
41
42
43
44
45
46
47
48
49
50
51
52
53
54
55
56
57
58
59
60

cells/mL with a detection limit of 430 cells/mL (S/N =3). The linear regression equation is $-\Delta f = 69.392 \log c - 168.577$ (where Δf is QCM frequency intensity and c stands for the concentration of MCF-7 cells), and the correlation coefficient of $R^2=0.9984$. The results demonstrated that the proposed method could be used to detect MCF-7 concentration quantitatively. Compared to other methods based on QCM technique,^{6, 17} this proposed QCM cytosensors had a relative wider linear range and lower detection limit.

3.4. Selectivity and specificity of the biosensor

In order to explore the selectivity of the present biosensor, contrast experiments were performed (Fig. 5). Erythrocyte, endothelial cell (HUVEC) and oral epithelial cell H376 were used as interfering substance to evaluate the selectivity and specificity of the proposed cytosensor. As shown in Fig. 5, the adsorptions of erythrocyte, HUVEC and H376 on CS-FA conjugation are all negligible with cells concentrations even up to 1.0×10^4 cells/mL. By contrast, the binding of CS-FA with 1.0×10^3 cells/mL MCF-7 cell resulted in much larger frequency shifts. Moreover, significant frequency shift was observed in the mixture of 1.0×10^3 cells·mL⁻¹ of erythrocytes, endothelial cell, oral epithelial cells and MCF-7 cells, respectively. These results demonstrate that the CS-FA modified QCM biosensor is highly specific for MCF-7 cells.

Fluorescence microscopy was used to characterize the CS-FA cytosensor for the recognition of MCF-7 cells because they could express high levels of FR.⁴² Low-toxic calcein-AM was chosen to carry out staining experiment for the determination of cell viability since its fluorescence intensity was proportional to the amount of live cells.^{35, 43} As shown in Fig. 6A, homogeneous fluorescence was observed when the electrode was exposed none cells. After the CS-FA/ITO was incubated into the solution with MCF-10 cells for 2 h, weak fluorescence could be observed (Fig. 6B), meaning few viable cells were adhere on the CS-FA film. However, strong fluorescence was observed after incubation into MCF-7 cells for 2 h (Fig. 6C), the attached round cells almost adhered and spreaded to irregular shapes on the surface of the film, indicating a good viability. Thus the CS-FA cytosensor did not

1
2
3 show cytotoxicity and was suitable for the immobilization of cells with good
4 biocompatibility and specificity.
5

6 7 3.5. Regeneration, reproducibility and stability of the cytosensor 8

9 The QCM-D chip after the recognition of MCF-7 cancer cells was regenerated
10 by rinsing the surface firstly with 0.2 M lysozyme at pH 6 for 2 h, this resulted in a
11 completely chitosan degradation into *N*-acetyl glucosamine, lysozyme and *N*-acetyl
12 glucosamine were then removed from the chip surface by treatment with PBS (pH
13 7.4). After modified the gold electrode and exposure to MCF-7 cells, the QCM
14 biosensor could again capture cells. As shown in Fig.7, after 5 cycles, the Δf values
15 still remained 83%. The results from five cycles indicate that the chitosan-based
16 QCM biosensor interface is biodegradability, sensing surface is reusable. The
17 regeneration method is superior to other methods,⁴⁴ which is due to the favorable
18 biological properties of chitosan such as biodegradability, biocompatibility, low
19 toxicity, as well as reasonable cost. The reproducibility of the QCM biosensor was
20 estimated by determining the cells level with three cytosensors of different batches
21 under the same experiment conditions. The relative standard deviation (RSD) of the
22 inter-assay was 7.28% at the cells concentration of 1.0×10^4 cells mL⁻¹, indicating
23 acceptable precision and fabrication reproducibility. The cytosensor retained its QCM
24 response after 2 weeks at 4 °C, without obvious decline. This indicated that the CS-FA
25 modified gold electrode was efficient to hold its stability and bioactivity as well.
26
27
28
29
30
31
32
33
34
35
36
37
38
39
40
41

42 3.6. Analysis of standard spiked blood sample 43

44 To verify to the preliminary validity of the present biosensor in complex matrix,
45 this CS-FA modified QCM system was applied for determination of MCF-7 in
46 standard spiked blood sample. For dilution fold of 5, 10 and 20, the obtained
47 recoveries for MCF-7 (1×10^4 cells/mL) in spiked blood were 119%, 115% and 108%
48 with corresponding relative standard deviation (n=3) of 11%, 8% and 6%, respectively.
49 This result suggests that the CS-FA modified QCM biosensor exhibits satisfactory
50 analytical ability towards cancer cell over-expressed FR in blood sample.
51
52
53
54
55
56
57
58
59
60

4. Conclusions

An effective strategy for the preparation of CS-FA with high biocompatibility and specificity was developed, and it could be used to fabricate a QCM biosensor for label-free MCF-7 breast cancer cell detection. The cytosensor when functionalized with FA as a target anchorage to capture MCF-7 cells specifically exhibited desirable performance for cancer cells detection. Therefore, we anticipate that this research will further facilitate the application of functionalized chitosan for biosensing applications and provide a convenient platform for clinical diagnoses in the future.

Acknowledgements

This work was supported by grants from National Natural Science Foundation China (No. 21375048), the Major State Basic Research Development Program of China (973 Program) (No. 2010CB833603).

References

1. Y.-F. Chang, S.-H. Hung, Y.-J. Lee, R.-C. Chen, L.-C. Su, C.-S. Lai and C. Chou, *Analytical Chemistry*, 2011, **83**, 5324-5328.
2. A. Jemal, F. Bray, M. M. Center, J. Ferlay, E. Ward and D. Forman, *CA: a cancer journal for clinicians*, 2011, **61**, 69-90.
3. N. Berois, M. Varangot, C. Sonora, L. Zarantonelli, C. Pressa, R. Lavina, J. L. Rodriguez, F. Delgado, N. Porchet, J. P. Aubert and E. Osinaga, *International Journal of Cancer*, 2003, **103**, 550-555.
4. H. Yin, Y. Zhou, C. Chen, L. Zhu and S. Ai, *Analyst*, 2012, **137**, 1389-1395.
5. L. Dumartin, H. J. Whiteman, M. E. Weeks, D. Hariharan, B. Dmitrovic, C. A. Iacobuzio-Donahue, T. A. Brentnall, M. P. Bronner, R. M. Feakins, J. F. Timms, C. Brennan, N. R. Lemoine and T. Crnogorac-Jurcevic, *Cancer Research*, 2011, **71**, 7091-7102.
6. Y. Pan, M. Guo, Z. Nie, Y. Huang, C. Pan, K. Zeng, Y. Zhang and S. Yao, *Biosensors & Bioelectronics*, 2010, **25**, 1609-1614.
7. M. Yan, G. Q. Sun, F. Liu, J. J. Lu, J. H. Yu and X. R. Song, *Anal. Chim. Acta*, 2013, **798**, 33-39.
8. C. Hu, D.-P. Yang, Z. Wang, L. Yu, J. Zhang and N. Jia, *Analytical chemistry*, 2013, **85**, 5200-5206.
9. C. Hu, D.-P. Yang, Z. Wang, P. Huang, X. Wang, D. Chen, D. Cui, M. Yang and N. Jia, *Biosensors and Bioelectronics*, 2013, **41**, 656-662.
10. C. Hu, D.-P. Yang, K. Xu, H. Cao, B. Wu, D. Cui and N. Jia, *Analytical chemistry*, 2012, **84**, 10324-10331.
11. C. Hu, D.-P. Yang, F. Zhu, F. Jiang, S. Shen and J. Zhang, *ACS applied materials & interfaces*, 2014.
12. S. Zhang, L. Zhang, X. Zhang, P. Yang and J. Cai, *Analyst*, 2014, **139**, 3629-3635.
13. J. Camps, I. Ponsa, M. Ribas, E. Prat, J. Egozcue, M. A. Peinado and R. Miro, *Faseb Journal*, 2005, **19**, 828-847.
14. Y. Fu, D. Lu, B. Lin, Q. Sun, K. Liu, L. Xu, S. Zhang, C. Hu, C. Wang, Z. Xu and W. Zhang, *Analyst*, 2013, **138**, 7016-7022.
15. N. Shao, E. Wickstrom and B. Panchapakesan, *Nanotechnology*, 2008, **19**.
16. A. Weltin, K. Slotwinski, J. Kieninger, I. Moser, G. Jobst, M. Wego, R. Ehret and G. A. Urban, *Lab on a Chip*, 2014, **14**, 138-146.
17. W. Shan, Y. Pan, H. Fang, M. Guo, Z. Nie, Y. Huang and S. Yao, *Talanta*, 2014, **126**, 130-135.
18. R. Hao, D. Wang, X. e. Zhang, G. Zuo, H. Wei, R. Yang, Z. Zhang, Z. Cheng, Y. Guo and Z. Cui, *Biosensors and Bioelectronics*, 2009, **24**, 1330-1335.
19. M. Guo, J. Chen, Y. Zhang, K. Chen, C. Pan and S. Yao, *Biosensors & Bioelectronics*, 2008, **23**, 865-871.
20. B. Thierry and H. J. Griesser, *Journal of Materials Chemistry*, 2012, **22**, 8810-8819.
21. T. W. Chung, Y. C. Tyan, R. H. Lee and C. W. Ho, *Journal of Materials Science-Materials in*

- 1
2
3
4
5
6
7
8
9
10
11
12
13
14
15
16
17
18
19
20
21
22
23
24
25
26
27
28
29
30
31
32
33
34
35
36
37
38
39
40
41
42
43
44
45
46
47
48
49
50
51
52
53
54
55
56
57
58
59
60
- Medicine*, 2012, **23**, 3067-3073.
22. K. A. Marx, T. Zhou, A. Montrone, D. McIntosh and S. J. Braunhut, *Analytical Biochemistry*, 2007, **361**, 77-92.
23. M. Tarantola, E. Sunnick, D. Schneider, A.-K. Marel, A. Kunze and A. Janshoff, *Chemical Research in Toxicology*, 2011, **24**, 1494-1506.
24. G. Garai-Ibabe, R. Grinyte, E. I. Golub, A. Canaan, M. L. de la Chapelle, R. S. Marks and V. Pavlov, *Biosensors & Bioelectronics*, 2011, **30**, 272-275.
25. M. Garcia-Fuentes and M. J. Alonso, *Journal of Controlled Release*, 2012, **161**, 496-504.
26. R. F. F. de Araujo, C. R. Martinez, K. P. D. Luna, R. M. C. Souza, D. Brunaska, R. F. Dutra and J. L. de Lima, *Applied Surface Science*, 2013, **274**, 33-38.
27. V. M. Esquerdo, T. R. S. Cadaval, Jr., G. L. Dotto and L. A. A. Pinto, *Journal of Colloid and Interface Science*, 2014, **424**, 7-15.
28. L. Zhao, Y. Hu, D. Xu and K. Cai, *Colloids and Surfaces B-Biointerfaces*, 2014, **119**, 115-125.
29. A. I. Neto, A. C. Cibrao, C. R. Correia, R. R. Carvalho, G. M. Luz, G. G. Ferrer, G. Botelho, C. Picart, N. M. Alves and J. F. Mano, *Small*, 2014, **10**, 2459-2469.
30. R. Li, C. Wang, Y. Hu, O. Zheng, L. Guo, Z. Lin, B. Qiu and G. Chen, *Biosensors & Bioelectronics*, 2014, **58**, 226-231.
31. S. Mansouri, Y. Cuie, F. Winnik, Q. Shi, P. Lavigne, M. Benderdour, E. Beaumont and J. C. Fernandes, *Biomaterials*, 2006, **27**, 2060-2065.
32. L. Zhang, F. Yang, J.-Y. Cai, P.-H. Yang and Z.-H. Liang, *Biosensors & Bioelectronics*, 2014, **56**, 271-277.
33. L. Tan, P. Lin, B. Pezeshkian, A. Rehman, G. Madlambayan and X. Zeng, *Biosensors & Bioelectronics*, 2014, **56**, 151-158.
34. J. Elsom, M. I. Lethem, G. D. Rees and A. C. Hunter, *Biosensors & Bioelectronics*, 2008, **23**, 1259-1265.
35. G. Yang, J. Cao, L. Li, R. K. Rana and J.-J. Zhu, *Carbon*, 2013, **51**, 124-133.
36. P. M. S. D. Cal, R. F. M. Frade, V. Chudasama, C. Cordeiro, S. Caddick and P. M. P. Gois, *Chemical Communications*, 2014, **50**, 5261-5263.
37. B. Ma, A. Qin, X. Li, X. Zhao and C. He, *International journal of biological macromolecules*, 2014, **64**, 341-346.
38. Y. Hu, B. Ma, Y. Zhang and M. Wang, *Biomedical Microdevices*, 2014, **16**, 487-497.
39. A. K. Agrawal, H. Harde, K. Thanki and S. Jain, *Biomacromolecules*, 2014, **15**, 350-360.
40. Y. Song, Y. Chen, L. Feng, J. Ren and X. Qu, *Chemical Communications*, 2011, **47**, 4436-4438.
41. V. Heitmann and J. Wegener, *Analytical Chemistry*, 2007, **79**, 3392-3400.
42. Y. Mi, Y. Liu and S.-S. Feng, *Biomaterials*, 2011, **32**, 4058-4066.
43. P. Grieshaber, W. A. Lagrèze, C. Noack, D. Boehringer and J. Biermann, *Journal of neuroscience methods*, 2010, **192**, 233-239.
44. Q. Chen, W. Tang, D. Wang, X. Wu, N. Li and F. Liu, *Biosensors & Bioelectronics*, 2010, **26**, 575-579.

Figure captions:

Scheme 1. (A) Schematic diagram of the experimental set-up. (B) The schematic representation of the label-free QCM biosensor for on-line detection of MCF-7 cancer cell. (C) Fluorescent image of the biosensor after captured MCF-7 cancer cells.

Fig. 1. Representative images of AFM (A) and SEM (B) of CS-FA and CS films. The images of the control (glass slide) are also shown for the sake of comparison.

Fig. 2. (A) UV-Vis spectra and (B) FT-IR spectra of CS, FA and CS-FA. (C) Contact angle of bare Au electrode (a), CS/Au (b) and CS-FA/Au (c). (D) Time-dependent frequency (c and d) and dissipation (a and b) responses of the QCM biosensor. Profile ($650 \text{ s} < t < 2000 \text{ s}$) represents the recognition of $1.0 \times 10^3 \text{ cells} \cdot \text{mL}^{-1}$ MCF-7 cancer cells (a and d) and $1.0 \times 10^3 \text{ cells} \cdot \text{mL}^{-1}$ endothelial cells (b and c). Control curves show the responses resulted from PBS buffer solution.

Fig. 3. (A) UV-Vis spectra of FA solutions with different concentrations: (a) 10, (b) 15, (c) 20, (d) 25, (e) 30 $\mu\text{g/L}$, respectively. Inset: Calibration plot of concentration of FA against absorbance intensity. (B) Determination of the concentration of FA in different conjugate of CS-FA. The error bars represent the standard deviation (S.D.) of three measurements.

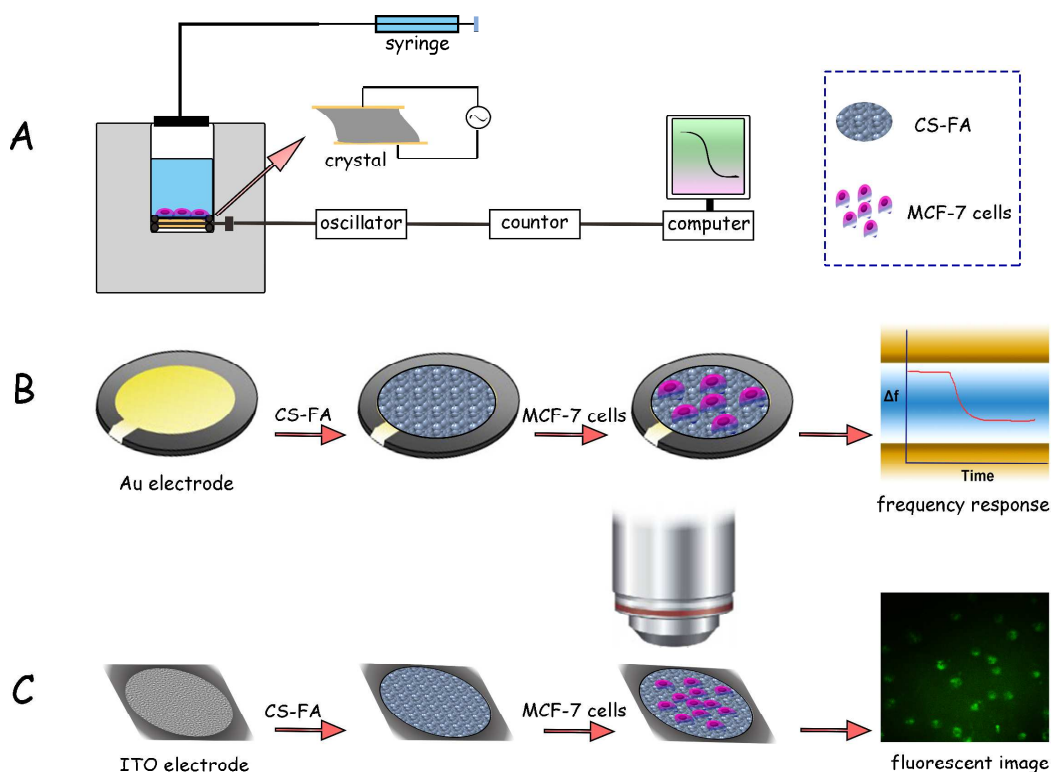
Fig. 4. Real-time frequency responses of the CS-FA modified QCM biosensor for MCF-7 cell. (a) 4.5×10^2 , (b) 1.25×10^3 , (c) 3.75×10^3 , (d) 4.05×10^4 , (e) 4.53×10^4 , (f) $1.01 \times 10^5 \text{ cells/mL}^{-1}$, respectively. Insets: The linear relationships between the frequency shifts and the logarithms of MCF-7 cells concentrations. The error bars represent the standard deviation (S.D.) of three measurements.

Fig. 5. Selectivity of the CS-FA modified QCM biosensor, (a) blank, (b) with $1.0 \times 10^4 \text{ cells} \cdot \text{mL}^{-1}$ of erythrocyte, (c) with $1.0 \times 10^4 \text{ cells} \cdot \text{mL}^{-1}$ of endothelial, (d) with $1.0 \times 10^4 \text{ cells} \cdot \text{mL}^{-1}$ of oral epithelial, (e) with $1.0 \times 10^3 \text{ cells} \cdot \text{mL}^{-1}$ of MCF-7, (f) with the mixture of $1.0 \times 10^4 \text{ cells} \cdot \text{mL}^{-1}$ of erythrocyte, endothelial, oral epithelial and MCF-7, respectively.

Fig. 6. Fluorescent images of the cells stained by calcein-AM after captured 2 h by the different interfaces: (A) The CS interface, (B) endothelial cells and (C) MCF-7 cells on the CS-FA interface.

Fig. 7. Frequency response of the chitosan-based QCM biosensor to 1.0×10^3 cells·mL⁻¹ of MCF-7 cells after regeneration cycles. The error bars represent the standard deviation (S.D.) of three measurements.

Figures:



Scheme 1.

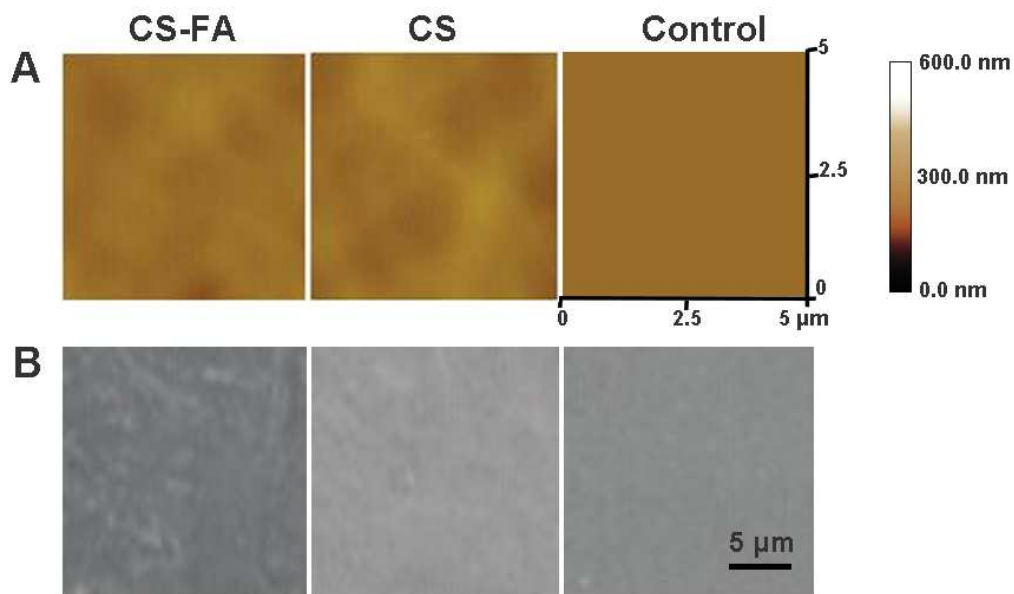


Fig. 1.

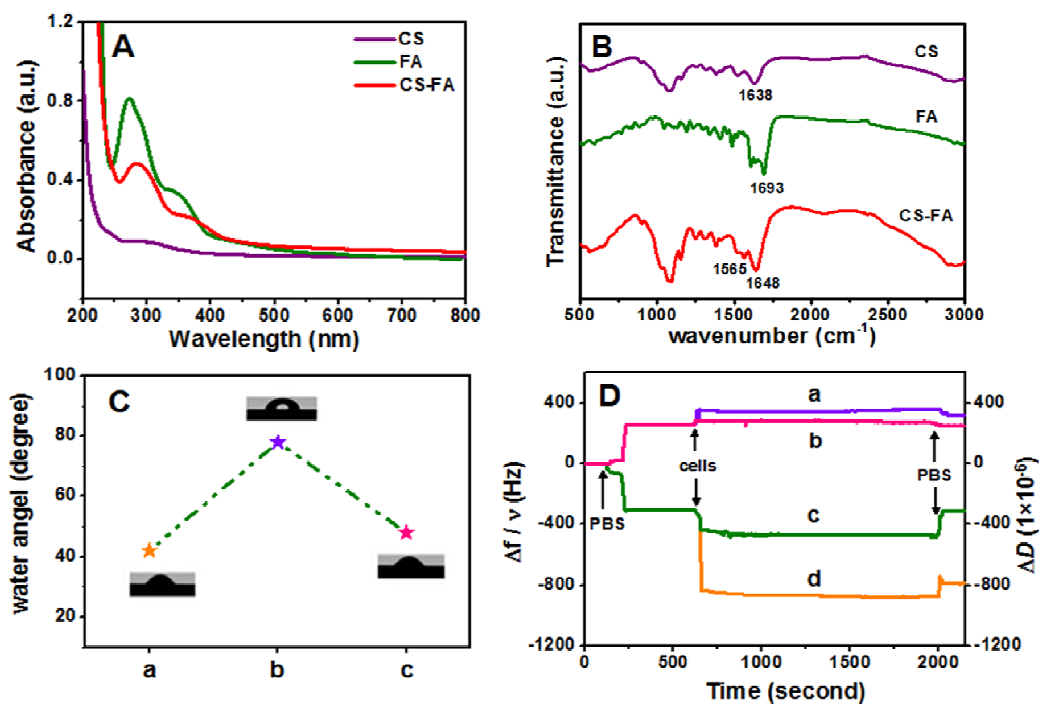


Fig. 2.

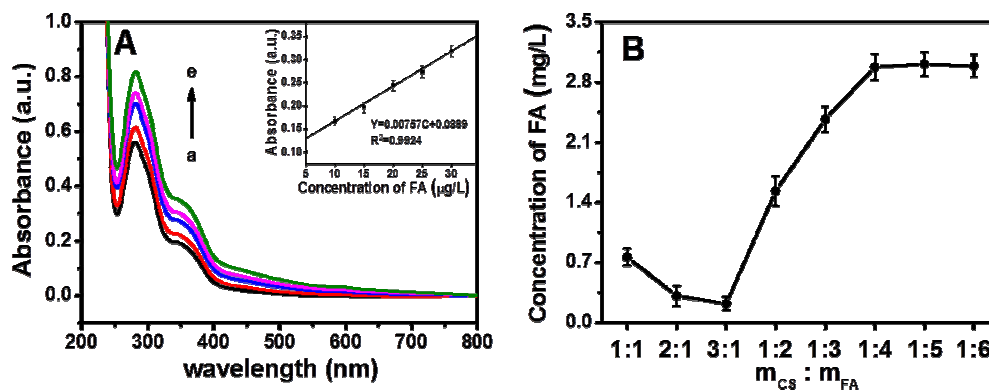


Fig. 3.

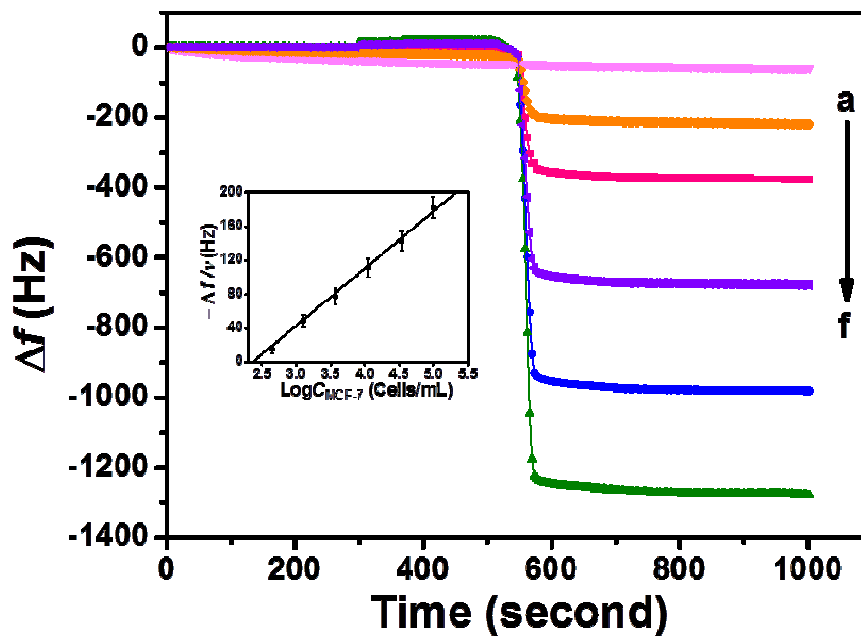


Fig. 4.

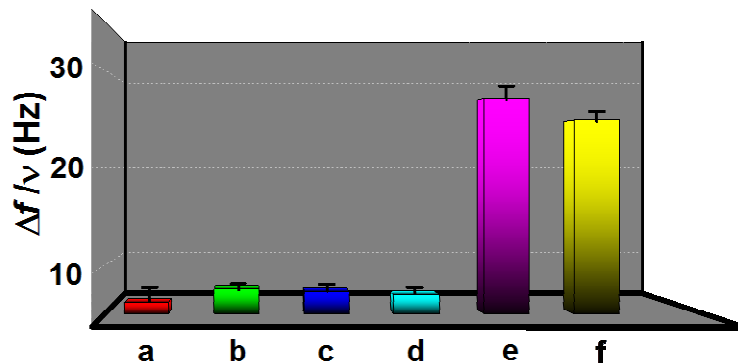


Fig. 5.

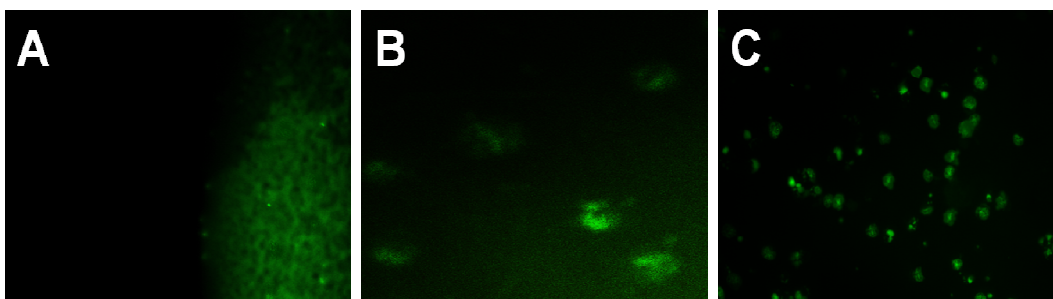


Fig. 6.

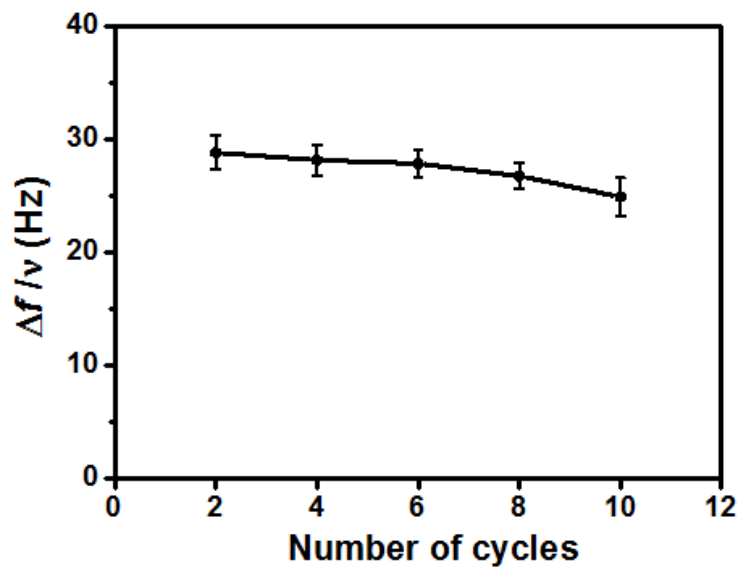


Fig. 7.